

# Organic cathode materials in sodium batteries

B. V. RATNAKUMAR, S. DI STEFANO, R. M. WILLIAMS, G. NAGASUBRAMANIAN,  
C. P. BANKSTON

*Jet Propulsion Laboratory, California Institute of Technology, 4800 Oak Grove Drive, Pasadena, California, USA 91109*

Received 17 July 1989; revised 11 September 1989

In order to circumvent the corrosion problems prevalent in many existing electrochemical couples using the Na/ $\beta''$ -alumina half cell, a new class of high energy density organic materials was studied as cathode materials. In particular, one material tetracyanoethylene (TCNE), has favourable electrochemical characteristics with a potential  $> 3.0$  V against  $\text{Na}^+/\text{Na}$  and energy density  $\sim 620$  Wh  $\text{kg}^{-1}$ . Adopting a cell designed to permit sealing the anode half cell, the performance of TCNE was evaluated under various experimental conditions, that is, at different concentrations of TCNE in the catholyte and with different current collectors. The electrochemical behaviour of the TCNE cathode and the kinetics of TCNE reduction were examined. The kinetic parameters, exchange current density and diffusion coefficient, were determined from different a.c. and d.c. electrochemical techniques and evaluated with respect to the changes in TCNE concentrations in the catholyte. A chemical transformation occurring in the cell operating conditions which does not reduce the electrochemical activity of TCNE was identified from FTIR spectra. Finally, possible approaches to the use of TCNE or other organic materials in sodium or lithium rechargeable batteries are outlined.

## 1. Introduction

Since the discovery in 1962 by Joseph Kummer and Neill Weber [1] that  $\beta''$ -alumina was a good sodium ion conductor, several studies have been made on its use as a solid electrolyte separator in various battery systems with liquid sodium as anode. The interest for many years has been focused on the sodium-sulphur battery [2] which has many attractive features such as high energy density ( $\sim 750$  Wh  $\text{kg}^{-1}$ ), high rate discharge capability permitted by a good (comparable to aqueous electrolytes) ionic conductivity of the  $\beta''$ -alumina solid electrolyte (BASE) at high temperatures, and long cycle life and life times. The cell operates typically at  $350^\circ\text{C}$  and energy densities typically of  $\sim 150$  Wh  $\text{kg}^{-1}$  have been demonstrated in finished cells [3]. However, there are certain difficulties associated with the use of sodium-sulphur batteries. In particular, due to the highly corrosive nature of sulphide melts, material selection for the current collector in the positive electrode is very critical and limited to few possible choices, for example, molybdenum, chromium, carbon and some super alloys [3]. Also, there is a likelihood of BASE degrading in polysulphide melts [4]. Further, the inherent violent reaction between liquid sodium and liquid sulphur demands a rather sophisticated design of the battery to circumvent the safety problem in the event of failure of the solid electrolyte ceramic.

Several alternative materials have been examined in the literature as positive electrodes, especially with chloroaluminate (mainly  $\text{AlCl}_3\text{-NaCl}$  melts) electrolytes. Interesting couples among these are  $\text{Na-SbCl}_3$  [5],  $\text{Na/Cl}_2$  [6],  $\text{Na/S}_2\text{Cl}_2$  [7], etc. Mamantov and

co-workers made a detailed study on  $\text{Na/S (IV) or } \text{SbCl}_3^+$  cells [8, 9]. These systems have attractive energy densities but are not free from corrosion problems. A new class of inorganic materials, that is, transition metal dichlorides, is gaining increasing attention as solid rechargeable cathodes in sodium batteries [10-13]. These systems can operate at lower temperatures  $\geq 150^\circ\text{C}$ ; the corrosion problems are proportionally less severe. The relatively sluggish kinetics of the chemical reaction between liquid sodium and catholyte reduces the safety problem considerably [14]. Also, the molten electrolyte  $\text{NaAlCl}_4$  remains invariant under normal discharge/charge, thus reducing polarization losses, localized current densities and failures therefrom. High energy densities ( $\sim 150$  Wh  $\text{kg}^{-1}$ ) were demonstrated with ferrous chloride and especially with nickel chloride. Studies are currently underway at JPL to evaluate other improved metal halides as cathode materials in sodium batteries for space applications.

In this paper, we report the use of organic materials as cathode depolarizers in high temperature sodium batteries to circumvent the problems of corrosion of the positive current collector/ $\beta''$ -alumina solid electrolyte. Carbonitriles with adjacent ethylenic bonds exhibit ready reducibility at high reduction potentials forming radical anions or charge transfer complexes and were therefore used as cathode depolarizers in primary batteries [15]. Tetracyanoethylene (TCNE), in particular, has a useful theoretical energy density, the theoretical energy density for the cell reaction involving a sodium anode and a TCNE cathode, that is,  $\text{Na} + \text{TCNE} \rightleftharpoons \text{Na-TCNE}$  is  $\sim 530$  Wh  $\text{kg}^{-1}$  based on the active materials and assuming a cell e.m.f. of 3.0 V.

The performance of TCNE as a cathode material in high temperature sodium rechargeable cells, its reduction kinetics at various proportions of catholyte (that is, depolarizer to molten electrolyte ratio), and the stability of TCNE at the temperatures of operation are discussed here.

## 2. Experimental details

The experimental set-up adopted for the Na-TCNE test cell is illustrated in Fig. 1. The cell essentially contains two metallic parts; the bottom, a stainless steel tube with a flange contains liquid sodium and acts as the negative terminal. The BASE tube (Ceramatec Inc.) separates the liquid anode and catholyte and is supported by its  $\alpha$ -alumina header resting on the metallic flange of the outer stainless steel tube. Inside the BASE tube is the mixture of molten electrolyte,  $\text{NaAlCl}_4$ , and cathodic depolarizer, TCNE, into which is immersed either a platinum or graphite foil to act as the working electrode and positive current collector. The top metallic half is bolted on to the metallic flange of the bottom portion with an aluminum o-ring placed between the plates. It is thus possible, in principle, to seal the anode (liquid sodium acting as counter electrode) half cell from the atmosphere, permitting the cell to be operated outside the glove box. The positive lead is connected to a metallic cap threaded into the top lid. A ceramic ring in the top lid prevents shorting between the metallic cap (positive terminal) at the top, and the bottom metallic half (negative terminal). The cell is heated electrically with a heating tape, wound around the bottom stainless steel tube, and its temperature is monitored with a thermocouple in contact with the tube. Thus the above electrochemical cell has a two-electrode configuration in the form of platinum/carbon working electrode and molten sodium counter electrode. However, the

necessity of a third (reference) electrode is not critical in this case, since the area of the counter electrode is relatively large, at least ten times that of the working electrode. Besides, the counter electrode, that is, liquid sodium/ $\beta''$ -alumina solid electrolyte interface, is known (from the polarization behaviour of sodium-sulphur batteries [16]) to be reactive and contribute little to any polarization losses in the measured electrode potentials, especially at the current densities employed in the present study. It is, therefore, reasonable to attribute the overall cell polarization/impedance to the working electrode alone under the present experimental conditions.

Conventional electrochemical equipment consisting of a 273 EG & G potentiostat/galvanostat, and a 5301 EG & G lock-in amplifier interfaced with an Apple 2E computer and a Soltec X-Y<sub>1</sub>Y<sub>2</sub> recorder/Epson printer was adopted. a.c. and d.c. measurements were carried out using EG & G a.c. Impedance and Soft-corr software. The kinetics parameters, especially exchange current density, were evaluated from a.c. impedance as well as d.c. methods, including linear polarization and potentiodynamic polarization. Diffusion coefficients were estimated from a.c. impedance data. Coulombic yields of TCNE were determined from galvanostatic discharges. Discharge/charge cycling was also carried out galvanostatically in a controlled fashion using the above electrochemical equipment.

All the chemicals, TCNE,  $\text{NaAlCl}_4$  as well as sodium were of analytical grade and were used as received. All the cell fabrication operations were carried out in an argon-filled glove box with oxygen concentration less than 10 ppm. The  $\beta''$ -alumina ceramic was cleaned by etching in hot phosphoric acid. The platinum electrode was cleaned in aqua-regia before each experiment.

## 3. Results and discussion

The electrochemical cell employed for these studies is analogous to the Na-metal chloride cell with a sodium/ $\beta''$ -alumina half cell and  $\text{NaAlCl}_4$  fused salt electrolyte but with a liquid cathode, TCNE. Its configuration may be represented as  $\text{Na(l)}/\beta''\text{-alumina}/\text{NaAlCl}_4\text{(m)} + \text{TCNE(m)}/\text{Pt or C}$ . The cell is typically operated at 230°C.

### 3.1. Cyclic Voltammetry

To establish the electrochemical window for the reduction of TCNE in the above cell configuration, and also to have an insight into the relative kinetics of the different processes involved in the reduction of TCNE, cyclic voltammetric curves were obtained at different scan rates of d.c. potential (Fig. 2). The voltammograms show reduction peak between 2.9–3.2 V against  $\text{Na}^+/\text{Na}$  and the conjugate oxidation peak around 3.6–3.8 V against  $\text{Na}^+/\text{Na}$ . The voltammetric peaks are not as sharp and the peak splitting is higher (in terms of electrode potential) as

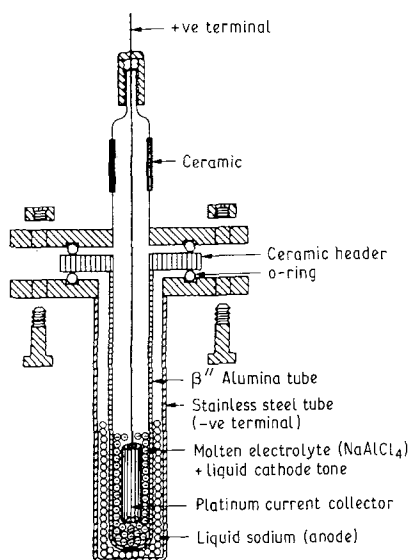


Fig. 1. Schematic representation of the electrochemical cell employed for the evaluation of TCNE comprising sodium anode, beta alumina solid electrolyte, TCNE in  $\text{NaAlCl}_4$  molten electrolyte and Pt or C current collector.

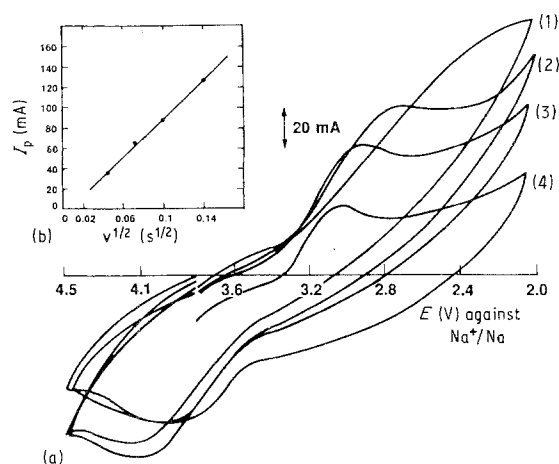


Fig. 2. (a) Cyclic voltammograms of TCNE in the Na/BASE/NaAlCl<sub>4</sub>, TCNE/Pt cell at 230°C at a scan rate of (1) 20, (2) 10, (3) 5, and (4) 2 mV s<sup>-1</sup>. (b) The peak current varies linearly with the square root of scan rate implying diffusion governed rate kinetics.

compared to a conventional diffusion governed process, which are primarily due to a high concentration (~10 W%) of the cathode depolarizer, TCNE in the molten electrolyte. The voltammograms indicate that the Na-TCNE cell could be operated between the limits of 2.0 and 4.0 V. In this range of potentials, the molten electrolyte is fairly stable as is evident from a low background current of  $< 100 \mu\text{A cm}^{-2}$  with the molten electrolyte alone (prior to the addition of TCNE) (curve not shown in the figure). At potentials below 2.0 V, aluminum deposition occurs whereas on the anodic side chlorine evolves at potentials  $\geq 4.0$  V. From the voltammograms at different scan rates, it is clear that the current attains a plateau at low scan rates, that is  $\leq 10 \text{ mV s}^{-1}$  which is more evident at lower scan rates. This suggests that the mass transfer processes control the kinetics of TCNE reduction, especially at high rates of reduction. A plot of peak current (plateau current) against the square root of the scan rate of potential is linear (Fig. 2), confirming the dominating role of mass transfer processes, possibly in the molten electrolyte, in the electrochemical reduction of TCNE.

### 3.2. d.c. polarization studies

In order to have qualitative as well as quantitative information on the kinetics of TCNE reduction, potentiodynamic curves (Fig. 3) were recorded at slow scan rates ( $0.5 \text{ mV s}^{-1}$ ) approximating steady state conditions. The current-potential curve shows the interference of mass transfer processes on the charge transfer kinetics. There is no well-defined linearity in the Tafel ( $E$  against  $\log I$ ) plots. Also, a limiting current is observed at high overpotentials (in the region of 500 mV) which may be ascribed to the slow rate of diffusion of the electroactive species, neutral and/or reduced TCNE. The limiting current is determined by the mass transfer conditions prevailing in the catholyte such as concentration and viscosity of catholyte, etc., and is typically  $1.5 \text{ mA cm}^{-2}$  in a catholyte

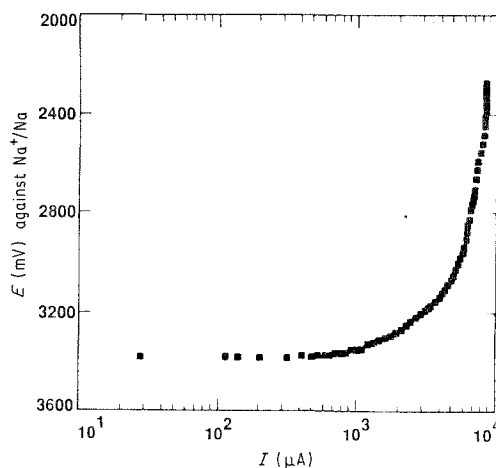


Fig. 3. Potentiodynamic polarization curve of TCNE in Na/BASE/NaAlCl<sub>4</sub>, TCNE (10 W%)/Pt cell at 230°C and at  $0.5 \text{ mV s}^{-1}$ .

containing 10 W% TCNE in NaAlCl<sub>4</sub>. Because of the strong interference of mass transfer processes on the charge transfer kinetics, it is not possible to calculate the kinetic parameters of TCNE reduction from the Tafel plot directly. A correction is therefore applied for the mass transfer polarization (interfacial concentration being different from the bulk concentration) in terms of the limiting current [17]. The corrected Tafel plot (Fig. 4) shows good linearity in the Tafel regime. The exchange current density for TCNE reduction is calculated from an extrapolation of the corrected Tafel plot to the equilibrium potential and the energy transfer coefficient obtained from its slope. The exchange current density and transfer coefficient for TCNE reduction are typically  $0.49 \text{ mA cm}^{-2}$  and 0.19 respectively on a Pt electrode in catholyte containing 10 W% TCNE in NaAlCl<sub>4</sub>.

The kinetic parameters for TCNE reduction were also obtained from the linear polarization method, wherein the electrode was polarized by  $\sim 15 \text{ mV}$  on either side of the equilibrium potential at a slower scan rate of  $0.05 \text{ mV s}^{-1}$ . At these low perturbations, the current potential equation is linearized resulting in a linear current potential curve, as observed

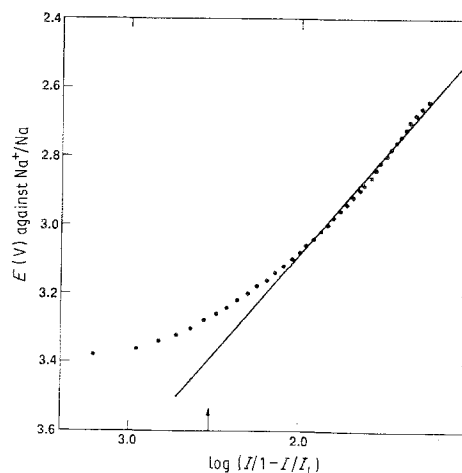


Fig. 4. Tafel plot corrected for mass transfer polarization of TCNE in Na/BASE/NaAlCl<sub>4</sub>, TCNE (10 W%)/Pt cell at 230°C (recast from Fig. 3),  $I_0 = 0.49 \text{ mA cm}^{-2}$ ,  $\alpha = 0.17$ .

experimentally. From the slope of the linear plot, the polarization resistance and hence exchange current density may be calculated. The exchange current density for TCNE reduction on the carbon electrode thus obtained is  $0.87 \text{ mA cm}^{-2}$  in a catholyte containing 10 W% TCNE in  $\text{NaAlCl}_4$ . The exchange current densities derived from linear polarization data are, in general, in good agreement with those calculated from corrected Tafel plots.

### 3.3 a.c. impedance

The a.c. impedance data were obtained by the lock-in technique in the upper frequency range (100 kHz–4 Hz) and by the Fast Fourier Transform (FFT) technique in the lower frequency range (10–0.01 Hz) with a peak-to-peak amplitude of 5 mV. The impedance data in the above two ranges were merged and recast into various graphical forms such as Nyquist, Bode and Randle's plots to derive qualitative as well as quantitative information on the kinetics of TCNE reduction. As mentioned in the experimental section, the impedance of the Na-TCNE cell may be totally attributed to the cathode alone under the present experimental conditions, due to the relatively large area of the anode and the low dynamic impedance of the  $\text{Na}/\beta''$ -alumina solid electrolyte interface. The Nyquist plot (Fig. 5) is a typical example of a charge transfer process coupled with mass transfer polarization. It contains a semi-circle in the high frequency range (100 kHz–50 Hz) attributed to the charge transfer process and a linear portion in the low frequency range (50–0.01 Hz) ascribed to the mass transfer impedance. The impedance behaviour may therefore be described, to a first approximation, by the Randle's equivalent circuit consisting of a series resistance,  $R_s$ , essentially due to the electrolytes (solid as well as molten), and a network of double layer capacitance parallel to a series combination of charge transfer resistance and Warburg (diffusion) impedance characterized by semi-infinite linear diffusion conditions. The slope of the linear portion in the Nyquist plot at low frequencies is slightly higher than unity and corresponds to a phase of  $58^\circ$ . This deviation may be attributed to the porosity (for example, sintered electrodes in Ni-Cd cells [18]), roughness of the carbon and etched platinum electrodes, or to the depression of the semi-circle corresponding to charge transfer process at high frequencies commonly observed in electrochemical systems involving solid electrolytes [19]. Based on the above equivalent circuit, the individual parameters, especially the charge transfer resistance, which gives the exchange current density for the reduction of TCNE, may be calculated. The charge transfer resistance is the difference between the low frequency and high frequency intercepts, whereas the high frequency intercept is the series resistance due to the electrolytes, as seen in the Nyquist plot (Fig. 5). The exchange current density and cell resistance thus obtained are  $1.8 \text{ mA cm}^{-2}$  and  $22.8 \text{ ohm cm}^2$  in a catholyte containing 10 W% TCNE in  $\text{NaAlCl}_4$ .

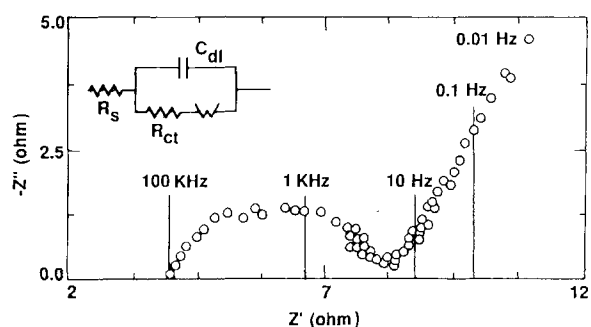


Fig. 5. Complex plane impedance plot of TCNE in Na/BASE/ $\text{NaAlCl}_4$ , TCNE (10 W%)/Pt cell at  $230^\circ \text{C}$ .

It is also possible to obtain information on the diffusion coefficient of TCNE in the catholyte from the a.c. impedance data. The slope of the Randle's plot (between the real (or imaginary) component of the impedance and the inverse square root of the angular frequency) gives the Warburg coefficient,  $\sigma$ , which, under the semi-infinite linear diffusion conditions assumed in the present case, is related to the diffusion coefficient as

$$\sigma = \frac{RT}{n^2 F^2 A \sqrt{2}} \left( \frac{1}{D_0^{1/2} C_0^*} + \frac{1}{D_R^{1/2} C_R^*} \right) \quad (1)$$

where  $A$  is the area of the electrode,  $n$  is the number of electrons involved in the reduction,  $D_0$  and  $D_R$  are diffusion coefficients of neutral and reduced TCNE and  $C_0^*$  and  $C_R^*$  are their corresponding concentrations in the bulk of the catholyte. In the situation where  $C_R^*$  is negligible, that is, when the catholyte contains no TCNE in the reduced form, it is reasonable to assume that the concentration polarization is essentially due to a slow approach of reactant to the electrode, rather than to a departure of the product therefrom. In other words, the second term in the above equation may be neglected and the diffusion coefficient of TCNE calculated. The diffusion coefficient of TCNE is of the order of  $10^{-9} \text{ cm}^2 \text{ s}^{-1}$  in a catholyte containing 10 W% of TCNE in  $\text{NaAlCl}_4$ .

### 3.4. Discharge/charge characteristics

The discharge/charge behaviour of TCNE and its reversibility are illustrated by a set of voltage-time curves during galvanostatic polarization at  $1 \text{ mA cm}^{-2}$  (Fig. 6). TCNE has a wide voltage range from 3.6 V to  $\sim 2.2 \text{ V}$  during discharge and from  $\sim 2.7$  to 3.8 V during charge. The discharge (as well as charging) curve of TCNE is sloping, as may be expected in a single-phase redox reaction involving soluble species. The equilibrium potential of TCNE also varies in a similar fashion with depth of discharge. It is therefore possible to estimate the state of charge of TCNE either from the equilibrium potential or the discharge potential.

The coulombic capacity delivered by the 45 mAh, positive-limited Na-TCNE cell with a TCNE concentration of 10 W% in  $\text{NaAlCl}_4$  is  $\sim 30 \text{ mAh}$ , which corresponds to a coulombic yield of  $\sim 65\%$  at  $1 \text{ mA cm}^{-2}$ . The coulombic capacities from curves 1

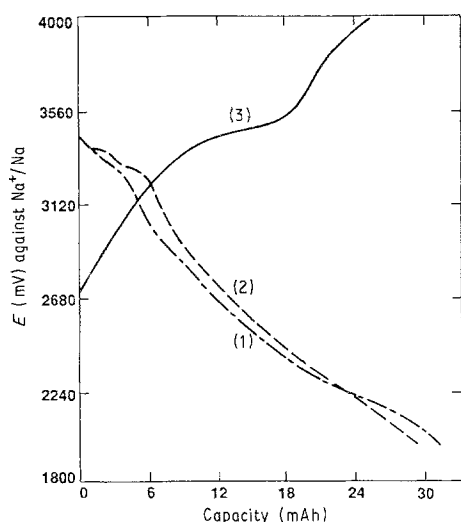


Fig. 6. Typical charge-discharge curves of TCNE in Na/BASE/NaAlCl<sub>4</sub>, TCNE (10 W%)/Pt cell at 230°C and at 1 mA cm<sup>-2</sup>: (1) fourth discharge, (2) fifth discharge, and (3) charge.

and 2 in successive discharges are similar, which demonstrates the reversibility of the Na-TCNE cell and rules out the possibility of any (irreversible) reactions involving fused salt electrolyte contributing to the coulombic capacity in the potential window of 2.0–4.0 V against Na<sup>+</sup>/Na.

### 3.5. Na-TCNE cell with different TCNE concentrations

Since the molten electrolyte NaAlCl<sub>4</sub> acts as a supporting electrolyte and would not contribute to the energy density of the battery, it is imperative that the concentration of TCNE in NaAlCl<sub>4</sub> needs to be increased to achieve higher energy densities. Cells with different concentrations of TCNE in the catholyte were therefore constructed and studied to characterize discharge performance as well as electrochemical kinetics.

A coulombic yield of 67% was obtained on a platinum foil electrode and ~60% was realized on a carbon electrode at 1 mA cm<sup>-2</sup> in catholytes containing 10 W% of TCNE in NaAlCl<sub>4</sub>. At higher concentrations of TCNE, say at 25%, the same coulombic yield was realized but at lower current density (0.25 mA cm<sup>-2</sup>) whereas at a current density of 1.5 mA cm<sup>-2</sup> the coulombic yield decreased to 40%. Thus it is clear that with increasing amounts of TCNE in the catholyte, the current efficiency for TCNE reduction drops. One needs to have a trade off between the (built in) energy density and the utilization efficiency or power capability in a TCNE battery.

Potentiodynamic polarization curves at higher concentrations of TCNE in the catholyte explain the poor current efficiency of TCNE with increasing TCNE concentration. The current-potential curves show a strong influence of mass transfer processes, in the Tafel regime at a TCNE concentration of 10 W% in NaAlCl<sub>4</sub>. At higher TCNE concentrations, however, the charge transfer kinetics become relatively sluggish as evidenced by increasing linearity in the Tafel

regime. The kinetics parameters obtained from the corrected Tafel plots also reflect the sluggish kinetics of TCNE reduction (Table 1). The exchange current density decreases by six and eight times as the concentration is increased to 25 W% and 37 W%, respectively. A similar trend is observed in the values of exchange current densities obtained from the linear polarization method at different TCNE concentrations (Table 1).

The a.c. impedance data indicate higher impedance of the cell with increased amounts of TCNE in the catholyte. The series resistance, which has significant contribution from the catholyte, is 2–6 times higher as the TCNE concentration is increased to 25–27 W% which may be expected from the poor conductivity of TCNE. The kinetic parameters, especially the exchange current density, show the same trend as those obtained from d.c. methods, that is the kinetics of TCNE reduction becoming sluggish at higher TCNE concentrations. The actual values of kinetic parameters obtained by a.c. methods are, however, about 4–5 times higher than the corresponding values from d.c. methods. This may be due to the assumptions involved in correcting for the polarization (especially mass transfer) losses in the d.c. methods. The diffusion coefficients of TCNE in the catholyte calculated from a.c. impedance data suggest a reduced mobility for TCNE in TCNE-rich catholytes. The diffusion coefficient decreases by two orders of magnitude as the concentration is raised to 25–37 W% and is of the order to 10<sup>-11</sup> cm<sup>2</sup> s<sup>-1</sup>. The lower diffusion coefficients may be responsible for the concentration polarization and hence for lower current efficiencies at higher TCNE concentrations.

It is thus clear from the a.c. and d.c. measurements with different TCNE concentrations that the reduction of TCNE is kinetically hindered by increased ohmic concentration as well as charge transfer polarization losses at higher TCNE concentrations in the catholyte.

### 3.6 Thermal instability of TCNE

At operating temperatures of around 230°C, TCNE undergoes an irreversible transformation forming a black adduct which does not melt. The kinetic hindrance to the reduction of TCNE observed in a.c. and d.c. studies could be related to this transformation of TCNE. The higher the amount of TCNE in the catholyte, the more viscous and resistive the catholyte becomes, resulting in higher polarization losses. TCNE is known to undergo a thermal reaction by itself though the presence of NaAlCl<sub>4</sub> might accelerate the transformation process. Even in a non-aqueous electrolyte, sulpholane/sodium tetrafluoro borate used in place of NaAlCl<sub>4</sub> in earlier studies, a similar phenomenon was observed at 150–200°C. More recently, Visco and DeJonghe also observed similar behaviour with TCNE (or with Tetracyanoquinodimethane, TCNQ) added in small quantity to organo-sulphur melts, especially tetraethyl thiuram disulphide (TETD) melts [20]. The TETD crystals darken at

Table 1. Electrochemical kinetic parameters obtained from various a.c. and d.c. measurements for the reduction of TCNE in Na/BASE/NaAlCl<sub>4</sub>, TCNE/Pt or E at 230°C with different concentrations of TCNE in the catholyte

System	Concentration	Cell capacity (cathode limited)	Coulombic yield	a.c. impedance data		d.c. polarization data				
				Cell resistance	Exchange current density	Diffusion coefficient	Linear	Tafel		
	(W %)	(mAh)		(ohms cm <sup>2</sup> )	(mA/cm <sup>2</sup> )	$\sigma$ ( $\Omega$ cm <sup>2</sup> s <sup>-1/2</sup> )	$D$ (cm <sup>2</sup> s <sup>-1</sup> )	$i_0$ (mA cm <sup>-2</sup> )	$i_0$ (mA cm <sup>-2</sup> )	$\alpha$
Pt	10	45	67% @ 1 mA cm <sup>-2</sup>	22.8	1.81	13.5	$1.0 \times 10^{-9}$	—	0.49	0.17
	37	150	—	80.9	0.53	24.0	$1.9 \times 10^{-11}$	0.075	0.06	0.24
C	10	60	60% @ 1 mA cm <sup>-2</sup>	29.4	3.3	4.8	$7.1 \times 10^{-9}$	0.87	0.65	0.51
	25	15	60% @ 0.25 mA cm <sup>-2</sup> 40% @ 1.5 mA cm <sup>-2</sup>	48.7	2.9	36.3	$2.0 \times 10^{-11}$	0.12	0.115	0.33

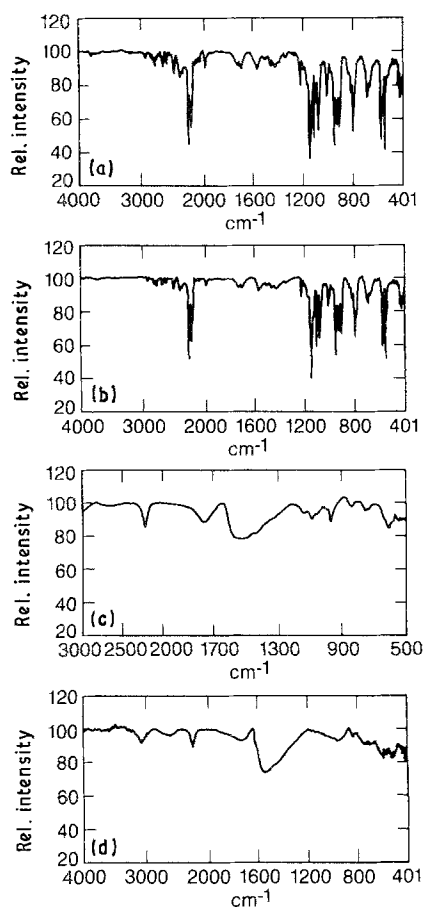


Fig. 7. FTIR spectra of TCNE under various experimental conditions: (a) reference, (b) heated, (c) heated together with  $\text{NaAlCl}_4$ , and (d) discharged in  $\text{Na/BASE/NaAlCl}_4$ , TCNE/Pt cell.

room temperature and eventually turn jet black at temperatures above  $74^\circ\text{C}$ . As a result of this 'charge transfer complex' formation, a hysteresis of the conductivity on cooling was also observed. Nevertheless, it is of interest to note that in the present case the electrochemical activity, at least corresponding to one electron per mole of TCNE, as well as the electrochemical reversibility are still retained in TCNE even after transformation, thus permitting it to be used as a rechargeable cathode material.

In order to understand the mechanism of the transformation, FTIR spectral studies were carried out on TCNE at various stages: that is, fresh TCNE, TCNE heated, a mixture of TCNE and  $\text{NaAlCl}_4$  after heating, and a mixture of TCNE and  $\text{NaAlCl}_4$  after heating and electrochemical reduction (discharge) (Fig. 7). The spectra were obtained on powdered samples in the diffuse reflectance mode. There appears to be no change in the FTIR spectrum of TCNE as a result of heating by itself, though physically the transformation seems to have occurred. The peaks around  $2200\text{--}2300\text{ cm}^{-1}$  assigned to  $\text{C}\equiv\text{N}$  as well as those around  $800\text{--}1000\text{ cm}^{-1}$  attributed  $\text{C}=\text{C}$  are also equally strong in the heated TCNE (Figs. 7a and 7b). The fine structure of TCNE is thus retained even after heating. However, there is considerable change in the spectral response after heating TCNE with  $\text{NaAlCl}_4$ . The sharp peaks around  $2200\text{--}2300\text{ cm}^{-1}$  are replaced by a single broad, less intense peak. Also, the multiple signals around  $800\text{--}1000\text{ cm}^{-1}$  corresponding to

ethylene bonds are conspicuously absent. Instead, a new broad peak around  $1500\text{ cm}^{-1}$  emerged in the TCNE heated with  $\text{NaAlCl}_4$  (Fig. 7c). This may be assigned to the  $\text{R}-\text{C}=\text{N}$ -group with a characteristic peak around  $1689\text{--}1487\text{ cm}^{-1}$  which might be present in the transformation product as a result of reduction of a cyanide group in TCNE. The spectrum of TCNE heated with  $\text{NaAlCl}_4$  remains the same after a nearly complete ( $\sim 70\%$ ) electrochemical reduction (Fig. 7d).

From the above observations, we may conclude that the transformation of TCNE at high temperatures is assisted by the presence of  $\text{NaAlCl}_4$ . The transformation is a result of a chemical reaction evidenced by a loss fine structure in the i.r. bands due to  $\text{C}\equiv\text{N}$  and  $\text{C}=\text{C}$  bonds and the emergence of a new peak due to partial reduction of the cyanide functional group. Nevertheless, the functional group responsible for the electrochemical activity is still available for reaction as evidenced by the spontaneous reduction occurring at the potentials corresponding to TCNE. However, there is a high degree of kinetic hindrance to the reduction, possibly due to the steric hindrance posed by the transformation product. Combining these facts with the well known tendency of TCNE to polymerize thermally and more favourably in the presence of donors, it is reasonable to conclude that there is a 'polymerization' occurring in TCNE under the experimental conditions, and hence its physical properties are altered, but the electrochemical behaviour remains similar.

#### 4. Summary

The use of organic materials as high energy density rechargeable cathodes in sodium batteries with  $\beta''$ -alumina solid electrolyte and  $\text{NaAlCl}_4$  molten electrolyte was demonstrated with a typical candidate material, tetracyanoethylene (TCNE). The reduction of TCNE occurs around  $3.0\text{ V}$  against  $\text{Na}^+/\text{Na}$  and is reversible. The exchange current density on either a carbon or platinum current collector is of the order of  $10^{-3}\text{ A cm}^{-2}$  in  $10\text{ W}\%$  catholyte mixtures. The kinetics of TCNE reduction are essentially governed by the rate of mass transfer in the catholyte. In TCNE-rich catholyte mixture, there is a kinetic hindrance to the reduction of TCNE as evidenced by increased polarization (ohmic, concentration as well as charge transfer) losses. The sluggish kinetics at higher TCNE concentrations are related to the transformation processes occurring in TCNE at the operating temperatures of  $\sim 230^\circ\text{C}$ , forming an adduct. FTIR studies point to a possible polymerization under the experimental conditions. Due to the sluggish kinetics at higher TCNE concentrations, it may not be possible to achieve high power densities from TCNE. The present studies indicate that TCNE is a candidate cathode material for low to medium power applications. Finally, it may be possible to use other stable high energy density organic materials in the above configuration, that is,  $\text{Na}(\ell)/\text{BASE}/\text{molten electrolyte} + \text{depolarizer}/\text{current collector}$  or TCNE

in ambient temperature, lithium batteries with non-aqueous TCNE-insoluble (excluding 2 Me-THF, sulphur, etc.) electrolytes to achieve high energy densities at power densities comparable to the practical systems.

### Acknowledgements

The work described here was carried out at the Jet Propulsion Laboratory, California Institute of Technology, under contract with the National Aeronautics and Space Administration. One of the authors (B. V. Ratnakumar) acknowledges the National Research Council for providing his Research Associateship during this work.

### References

- [1] J. T. Kummer and N. Weber, *Proc. SAE Congr.*, (1967), Paper 670179.
- [2] J. L. Sudworth and A. R. Tilley, 'The Sodium Sulphur Battery', Chapman and Hall Ltd., New York, (1985) and references therein.
- [3] R. P. Tischer, 'The Sulphur Electrode', Academic Press, New York, (1983).
- [4] M. Liu, 'Degradation of Sodium  $\beta$ " Alumina Electrolyte in Contact with Sulfur/Sodium Polysulfide Melts', Lawrence Berkeley Laboratory, Report (1986) LBL-21563; see *Energy Abstr.*, (1986), **11** (32), Abstr. no. 50849.
- [5] N. P. Yao and J. R. Selman, 'Proc. Symp. Load Levelling', ECS, Princeton, NJ, (1977).
- [6] J. J. Werth, U.S. Patent 3 847 667 (1974); U.S. Patent 3 877 984 (1975).
- [7] J. J. Auburn and S. M. Granstaff, Jr., *J. Energy* **6** (1982) 86-90.
- [8] G. Mamantov, R. Marassi, M. Matsunga, Y. Ogata, J. P. Wiaux and E. J. Frazer, *J. Electrochem. Soc.* **127** (1980) 2319.
- [9] G. Mamantov, 'Rechargeable High-Voltage Low-Temperature Molten-Salt Cell Na/ $\beta$ " Alumina/SCl<sub>3</sub><sup>+</sup> in AlCl<sub>3</sub>-NaCl', Final report for Lawrence Berkeley Laboratory, LBL-21653, (December 1985).
- [10] J. Coetzer, R. J. Bones, R. C. Galloway, D. A. Teagle and P. T. Moseley, U.S. Patent 4 546 055 (1985).
- [11] J. Coetzer, *J. Power Sources* **18** (1986) 377.
- [12] R. C. Galloway, *J. Electrochem. Soc.* **134** (1987) 256.
- [13] R. J. Bones, J. Coetzer, R. C. Galloway and D. A. Teagle, *J. Electrochem. Soc.* **134** (1987) 2379.
- [14] R. J. Wedlake, A. R. Tilley and D. A. Teagle, *Bull. Electrochem.* **4** (1988) 41.
- [15] W. R. Wolfe, Jr., U.S. Patent 3 081 204, (1963).
- [16] For example, R. J. Bones and T. L. Markin, *J. Electrochem. Soc.* **125** (1978) 1587.
- [17] K. J. Vetter, 'Electrochemical Kinetics' Academic Press, New York (1967), Chapter 2.
- [18] S. Sathyanarayana, S. Venugopalan and M. L. Gopikanth, *J. Appl. Electrochem.* **9** (1979) 125.
- [19] H. J. de Bruin and A. D. Franklin, *J. Electroanal. Chem.* **119** (1981) 405.
- [20] S. J. Visco and L. C. DeJonghe, *J. Electrochem. Soc.* **135** (1988) 2905.